SC-5308 – Structure and dynamics of supercooled fumed silica suspensions

Fabio Giavazzi,[1] Stefano Aime,[2] Phillippe Bourrianne,[2] Roberto Cerbino,[3]
William Chevremont,[4] Eric Freyssingeas,[5] and Thomas Gibaud[5]

[1] *Milan*
[2] *ESPCI*
[3] *Vienna*
[4] *ESRF*
[5] *Univ Lyon, Ens de Lyon, Univ Claude Bernard, CNRS, Laboratoire de Physique, F69342 Lyon, France*

(Dated: March 13, 2023)

Report on the run SC-5308 that took place at ID02 from the 31/01/2023 to the 03/02/2023.

Please be aware that for the moment the authors order is quite arbitrary and will need to be discuss later on in the process.

PACS numbers: xxx

I. INTRODUCTION

The glass transition is an out of equilibrium transition from the fluid to a disordered solid obtained at very high volume fractions. The glass transition is a dynamical arrested transition where colloids are trapped within the cage formed by their neighbors. The absence of rearrangement on long time scales leads to the solid behavior of the suspension. This transition has been well studied for hard-sphere colloids with experiments on model colloids [1], proteins [2] or theory [3, 4]. Here, we aim to study this transition for fractal colloids, namely fumed silica dispersed in a good solvent. This system presents two originalities compared to hard-sphere colloidal systems. As the volume fraction is increased, the system viscosity diverges at low volume fraction, $\sim$ 30% and the colloids interpenetrate each other. Using SAXS and XPCS, we will systematically explore the structure and dynamics of fumed silica dispersion as a function of their volume fraction. We aim to unravel the role of interpenetration in glass forming liquids.

Please find below a first draft of the analysis of the data. This is work in progress. There are still plenty of analysis to carry out.

II. MATERIALS AND METHODS

A. Fumed silica

Fumed silica particles come from the silicon tetrachloride pyrolysis. The fumed-silica particles are composed of nodules of a few nanometers that are fused together permanently during the flame synthesis and form aggregates of a few hundreds of manometers [**?**]. Those particles are widely used in the industry, such as shear thickening agents, light abrasives in toothpaste, to cite a few. Here, we use fumed silica AE300 from EVONIK INTL GROUP. The fumed silica come in powder and are dispersed in a good solvent at a weigh concentration c. The solvent is composed of 87%w of glycerol and 13%w of deionized water. The solvent is newtonien and has a viscosity of 123 mPa.s at $T = 20°$C. The fumed silica powder is dispersed using vigorous mixing during 10 min, then sonicated for 30 min at 50°C and finally degazed until the sample is homogeneous and translucent. For high concentrations the sample are eventually centrifuged to remove trapped air bubbles.

We designed the system so that the fumed silica dispersion is quasi entropic and that the sole control parameter is the volume fraction ϕ. To this end, we have index matched the dispersion to annihilate the van der Waals interactions: the index of refraction of the water glycerol mixture $n_{wg} = xxx$ and the one of fumed silica is $n_{fs} = xxx$. To check the entropic nature of the system, we have checked the properties of the system varying the temperature and the addition of sodium chloride. Both parameters displays mild change on the system properties as reported in the appendix IV

We have prepared suspensions at various volume fractions ϕ by varying the mass concentration c: $\phi = \frac{c}{\left(c+\frac{d_{fs}}{d_{bck}}(1-c)\right)}$ where $d_{fs} = 2.0$ is the density of the fumed silica particles [**?**] and $d_{bck} = 1.226$ is the density of the solvent at 20°C.

B. Rheology

we used a rheometer to measure the mechanical properties of fumed silica dispersion. We carried out our experiments with the stress-controlled rheometers MCR301 (Anton Paar) equipped with a rough cone (radius 40 mm, angle 1°) and a smooth rough plate both made of steel. We performed flow curves and oscillatory tests. The flow curve were obtained by increasing the stress from $\sigma = 0.1$ Pa up to a few hundreds or few thousand pascal depending on the sample and measuring the resulting shear rate $\dot{\gamma}$ or viscosity η. The oscillatory tests were carried out at $f = 0.1$ Hz with increasing strain amplitude γ and we retrieved the stress and the real part of the

complex viscosity η'. In such conditions, both method give identical flow curves: $\eta' = \eta = funct(\sigma)$.

C. SAXS and XPCS

William could you please rewrite this section

The microstructural and dynamical properties of the fumed silica dispersion are investigated using XPCS and SAXS on the ID02 beamline at the European Synchrotron Radiation Facility (ESRF, Grenoble, France) [**?**]. The samples were injected is borosilica capillary (WJM xxx) of diameter 1.5mm. The incident X-ray beam of wavelength xxx 0.1 nm is collimated to a vertical size of 50 μm and a horizontal size of 100 μm. The 2D scattering patterns were measured using an Eiger2 4M pixel array detector and the subsequent data reduction procedure is described elsewhere [**?**]. The scattering intensity $I(q)$ is obtained by subtracting the two-dimensional scattering patterns of the fumed silica dispersion and the background solvent. The resulting scattering intensity presented in this article always remained isotropic. Therefore, we radially averaged the normalized intensity pattern to obtain one dimensional $I(q)$.

xpcs setup xxx

XPCS experiments, sequential acquisitions from the same sample spot are measured, so that the intermediate scattering function $g_1(q, \Delta t)$ (ISF) can be calculated from the scattered intensity $I(\overrightarrow{q})$ as $g_2(q, \Delta t) = \langle I(\overrightarrow{q}, t) I(\overrightarrow{q}, t + \Delta t) \rangle / \langle I(\overrightarrow{q}) \rangle = 1 + \beta g_1(q, \Delta t)^2$. β is the speckle contrast. The time delay between two consecutive time frames is denoted Δt and $\langle \dots \rangle$ is the ensemble average over all equivalent delay times t and pixels within a certain range of the absolute value of q. We probed the properties of the ISF by acquiring movies at different frame rate and stitching the $g_2(q, \Delta t)$ so that Δt ranges from 1 ms to 10000 s.

III. RESULTS FOLLOWING OUR PRELIMINARY ANALYSIS OF THE DATA

A. Fumed silica form factor

The form factor $I_{FF}(q)$ of fumed silica AE300 was measured at $c = 0.3\%_w$ and is displayed in Fig. 1. $I_{FF}(q)$ displays two distinct breaks in log-log representation, corresponding to the radius a_0 of gyration of the primary particles, and the radius a of gyration of the clusters. Between these boundaries the scattering follows a power law related to the mass fractal dimension, D_m, while above the high-q boundary the scattering follows a power law related to the surface fractal dimension of the primary particles, D_s. The form factor is fitted by a mass surface fractal model [5]:

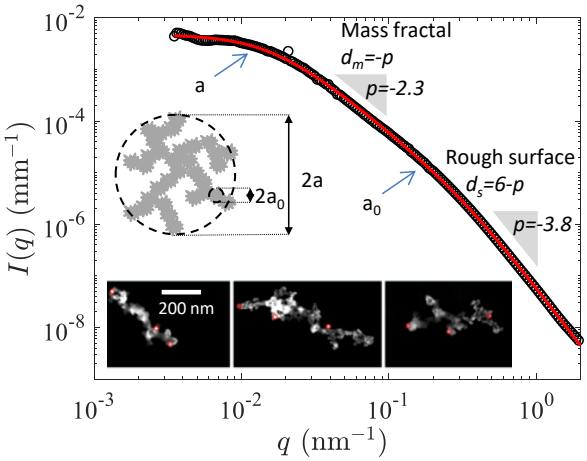

FIG. 1. Form factor of the fume silica AE300 at c=0.03%$_w$. The red line is a fit to the data following Eq. 1. Middle inset: sketch of the fumed silica. Lower inset: TEM images of the fumed silica adapted from [6].

$$I_{FF}(q) = \frac{I_0}{\left[1 + \frac{(qa)^2}{3d_m/2}\right]^{\frac{d_m}{2}}} \frac{1}{\left[1 + \frac{(qa_0)^2}{3(6-d_m-d_s)/2}\right]^{\frac{6-d_m-d_s}{2}}}. \quad (1)$$

This model yields $a = 117$ nm, $D_m = 2.3$, $a_0 = 4.5$ nm and $D_s = 2.2$. This model assumed that the primary particles and the cluster are monodisperse. This is not the case.

ToDo:
↦ Take into account the polydispersity
↦ Remake some TEM images and get some pdf of the size

B. Flow curves

The fumed silica dispersion show a peculiar rheological behavior. In Fig. 2a, we have plotted the relative viscosity η/η_{bck} as a function of the shear stress sigma for difference volume fraction ϕ. The η/η_{bck} increases with ϕ. Moreover, at high enough volume fractions, the dispersion is shear thinning at low σ and shear thickening at high σ. Repulsive colloid are expected to be shear thinning. Classically shear thickening is present when particles have a rough surface. This roughness tend to prevent the colloids from sliding or rolling path each other under shear and leads to an increase of viscosity. Here, we hypothesize that rather than the particle roughness it is the particle fractal nature which leads to interpenetration which is responsible for the shear thickening effect.

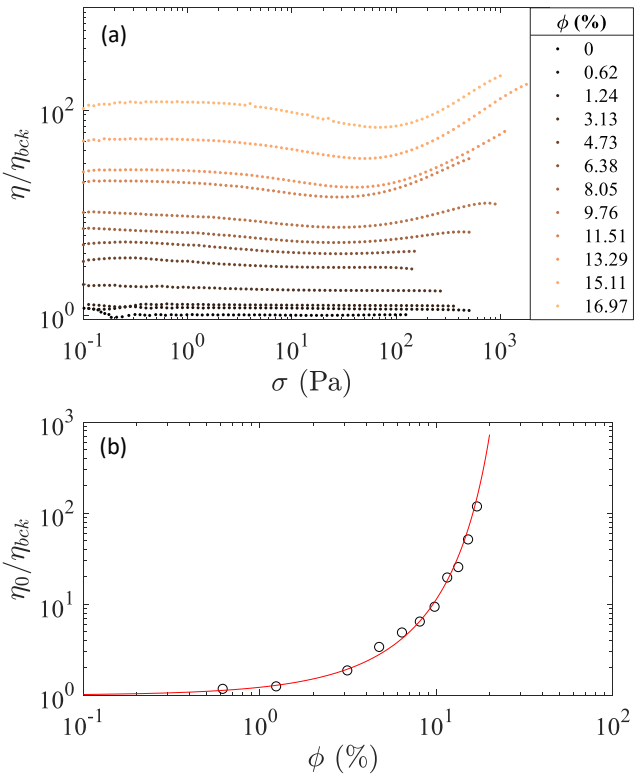

FIG. 2. Viscous properties of the fumed silica dispersion. a) Flow curves: evolution of the normalized viscosity η/η_{bck} as a function of the shear stress σ for different volume fraction ϕ. b) Evolution of the normalized zero shear viscosity as a function of ϕ. The red line is a fit to the data following the Krieger Dougherty relation, Eq. 2.

The zero shear relative viscosity which corresponds to the relative viscosity extrapolated at $\sigma = 0$ is displayed in Fig. 2b. We used Krieger–Dougherty relation to fit our data [7]

$$\eta/\eta_{bck} = (1 - \phi/\phi_g)^{\nu} \tag{2}$$

We find $\phi_g = 0.25$ and $\nu = 6$. As compared to hard sphere dispersion where $\phi_g = 0.58$ and $\nu = 2$ [8**?**], fumed silica dispersion form glass at much lower volume fraction and the diverging regime is much stiffer.

ToDo:
↦ viscosity measurements seem to cleaners in oscillatory modes at $f = 0.1Hz$. check and redo.

C. Structure

The scattering intensity $I(q)$ normalized by the volume fraction ϕ of the fumed silica dispersions in quiescent conditions is displayed in Fig. 3a. Qualitatively, the fumed silica dispersion display the typical features of a repulsive system: (i) as ϕ increases the low-q intensity decreases; (ii) the correlation peak move to high-q as ϕ increases; (iii) the correlation peak is very smooth probably due to polydispersity [9]. In Fig. 3b, using the form factor measured in Fig. 1, we have extracted the structure factor $S(q)$. In Fig. 3c, we have plotted $S(q \mapsto 0)$. As $q \mapsto 0$, we are in the thermodynamic limit and $S(0) = k_B T \partial\rho/\partial\Pi$ is an indirect measurement of the state equation of the fumed silica dispersion. In a first attempt to fit $S(q \mapsto 0)$, we considered the hard sphere model [2]:

$$S(0) = \frac{(1-\phi)^4}{(1+2\phi)^2 + \phi^3(\phi-4)} \tag{3}$$

As shown in Fig. 3c, the hard sphere model overestimate $S(q \mapsto 0)$. The experimental data points. The data point toward a glass transition around $\phi_g \simeq 0.3$.

Next, we extracted empirically from $S(q)$ the correlation peak position q_p such that $S(q_p) = 0.90$ and display q_p as function of ϕ in Fig. 3d. We observe two regimes. At low ϕ, $q_p \sim \phi^{1/3}$ in agreement with what is expected for a repulsive system. At $\phi > 6\%$, $q_p \sim \phi^{0.8}$. At $\phi \simeq 6\%$, $q_p \simeq 0.065$ nm^{-1} corresponds to an interparticle distance $2\pi/q_p \simeq 100$ nm. This distance is bit lower than the fumed silica diameter $2a = 234$ nm. Above $\phi \simeq 6\%$, the particle certainly interpenetrate. The fact that the power law exponent is 0.8 is however counter intuitive. We would have expected that it become harder to push particles closer together as they interpenetrate so that this exponent is lower than 1/3.

ToDo:
↦ Would it be useful to measure $I(q)$ at larger q to check if $S(q)$ really show to structure peak?
↦ understand the sharp increase of neighbour distance in Fig. 3.
↦ can we find a model to fit $S(q = 0)$? We have tried to model $S(0)$ using a monodisperse hard sphere model but it fails. Try polydisperse hard sphere [2]
↦ can we find a model to fit $S(q)$? Try polydisperse hard sphere [9]

D. Dynamics

In our preliminary analysis, we focused on two volume fractions: $\phi = 0.03$ and $\phi = 0.132$ The dynamics is obtained by XPCS and is shown in Fig. 5. We have fitted the intensity autocorrelation function g_2 either by a single or double exponential: $g_2(q, \Delta t) = 1 + \beta g_1^2$, with

$$g_1(q, \Delta t) = e^{-(\Gamma_1 t)^{\alpha_1}} \tag{4}$$

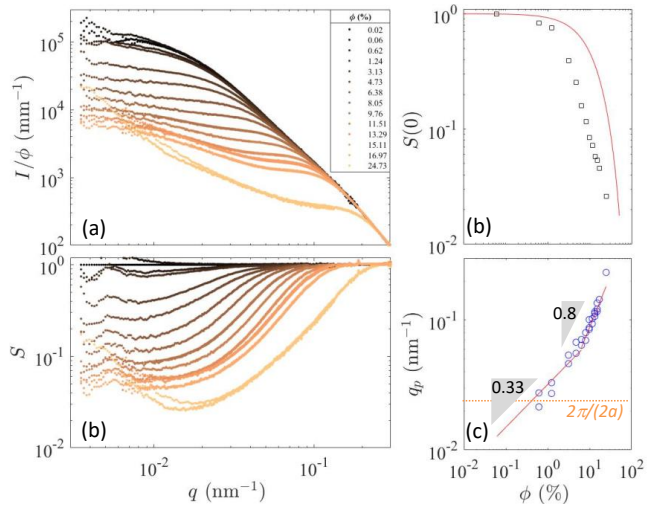

FIG. 3. a) Scattering intensity $I(q)$ normalized by the volume fraction ϕ of the fumed silica dispersions. b) Structure factor $S(q)$ for different ϕ. c) $S(q \mapsto 0)$. d) q_p as a function of ϕ. q_p is determined such that $S(q_p) = 0.90$. The red lines are guide to the eye: power law of exponent 0.33 and 0.8. The dash orange line corresponds the q related to the diameter of the FS particle.

$$g_1(q, \Delta t) = (1 - f)e^{-(\Gamma_1 t)^{\alpha_1}} + fe^{-(\Gamma_2 t)^{\alpha_2}} \qquad (5)$$

The stretch exponential allow us to consider a rate distribution with an average rate of

$$\langle \Gamma_i \rangle = \alpha_i \Gamma_i / GammaFunct(1/\alpha_i) \qquad (6)$$

In Fig. 4, we analysed the dynamics of a relatively dilute sample at $\phi = 0.06$. In Fig. 4a, g_2 is well fitted by a single exponential decay. There are little different between the non-stretched and stretched ($\alpha_1 \simeq 1$) single exponential fit. We oberve that the decay rate γ_1 is diffusive. The average diffusion coefficient is $D = mean(\Gamma_1/q^2) = 0.015$ μm/s. Following the stokes Einstein relation with find an hydrodynamic radius of $a_h = k_B T/(6\pi\eta_{bck} D) = 133$nm. The hydrodynamic to gyration radius ratio is $a_h/a = 1.14$ (xxx verify temperature in the hutch) a value a bit lower than what is expected for hard spheres: $\sqrt{(5/3)} = 1.3$.

In Fig. 5, we analysed the dynamics of a relatively concentrated sample at $\phi = 0.132$. In Fig. 5a, we observe two relaxation process: the β-relaxation on short time scale and the α-relaxation on long time scales as expected for a supercooled liquid. At high-q the β-relaxation is predominate is measure mostly the free diffusion of the particle. At high-q we observe both the α and β-relaxation as the particle may escape the cage formed by it neighbour particles.

The way we fit g_2 has consequences on the value of $\langle \Gamma_i \rangle$. In Fig. 5b, The long time rate Γ_2 is diffusive and mildly affected. However, the short time rate γ_1 is affected: when $\alpha_1 = \alpha_2 = 1$ it is almost ballistic. When α_1 and α_2 are set free, we observe in Fig. 5c that the α_i are

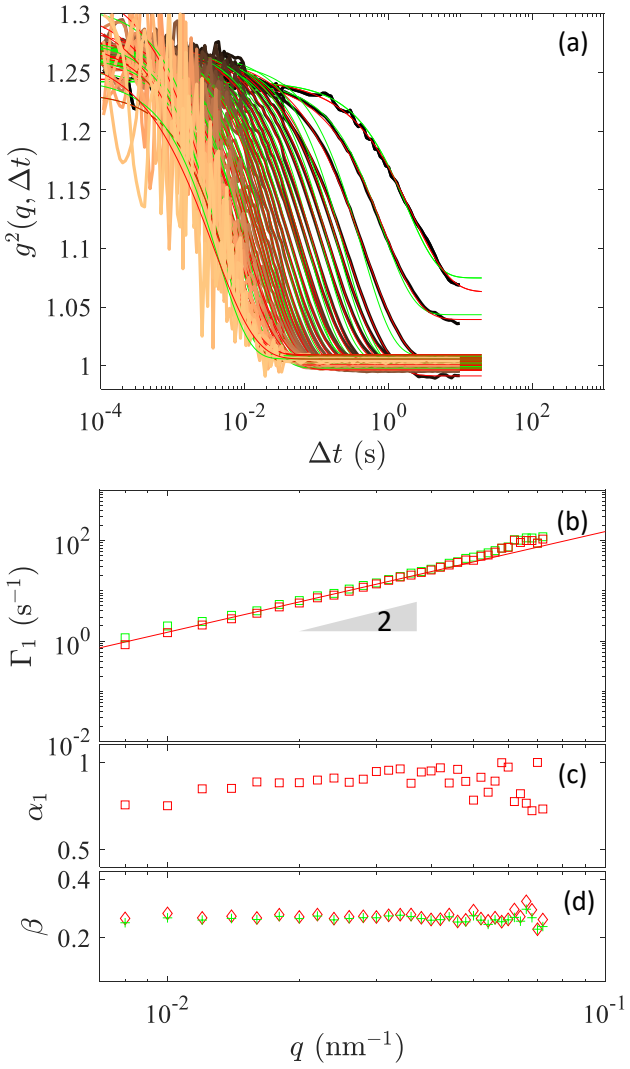

FIG. 4. Dynamics of fumed silica dispersion at $\phi = 0.6\%$. (a) g_2 as a function of Δt and q. green lines: simple exponential with $\alpha_1 = 1$. red lines: simple exponential (Eq. 4). Fit gives a diffusiv coefficient D =0.015 μm/s(b) Average rates. (c) Exponent α_1. (d) Ccoherence factor β.

inbetween 0.6 and 1. The non ergodic factor which indicate the plateau value between the β and α-relaxation decreases with q.

ToDo:
↦ Use the contin [10] algorithm to get the rates distribution and average values.
↦ Analyse the rest of the volume fractions.
↦ Compare the zero shear viscosity and the dynamics.
↦ Hydrodynamic function.

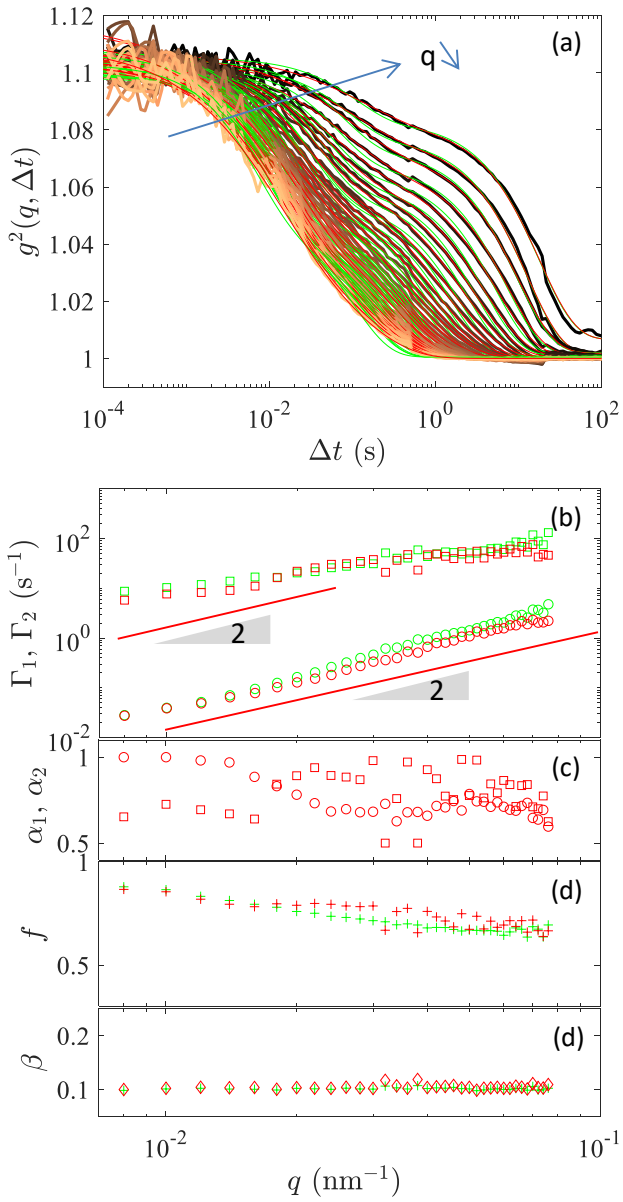

FIG. 5. Dynamics of fumed silica dispersion at $\phi = 13.2\%$. (a) g_2 as a function of Δt and q. green lines: double exponential with $\alpha_1 = \alpha_2 = 1$. red lines: double exponential (Eq. 5). (b) Average rates. (c) Exponent α_1 and α_2. (d) non ergodicity parameter f. (e) coehrence factor β.

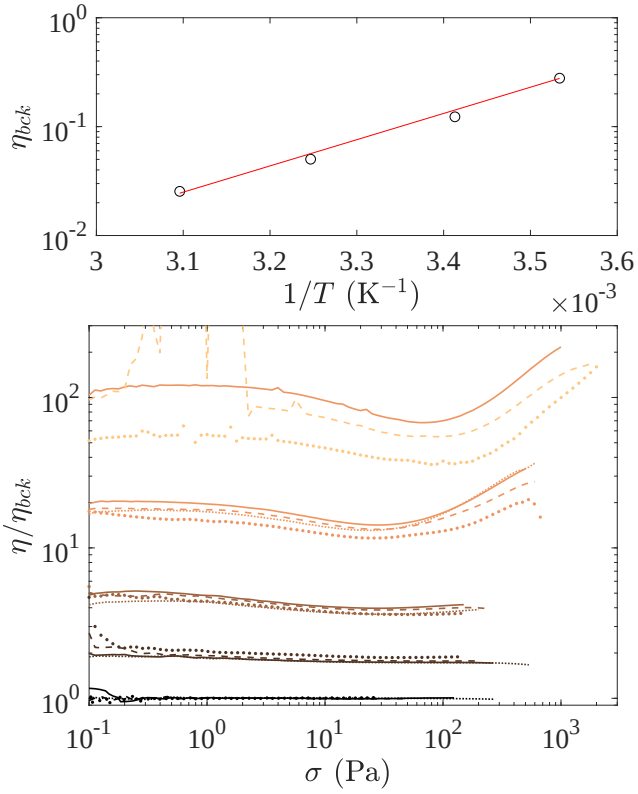

FIG. 6. Flow curves and temperature. (a) Viscosity of the background solvent as a function of $1/T$. The red line is an Arrhenius fit: $\eta = Ae^{B/T}$, with $A = 8.5.10^{-10}$ Pa.s and $B = 5550$ K (b) Normelized viscosity for $T = 10$ (:), 20 (-), 35 (- -) and 50 (.) °C. From bottom to top: $\phi = 0$, 0.03, 0.06, 0.115, 0.17.

IV. APPENDIX

A. Influence of the temperature

See Fig. 6

B. Influence of NaCl

See Fig. 7

C. Stitching the autocorrelation functions

D. Hard sphere model to fit $S(q)$

[1] G. Brambilla, D. El Masri, M. Pierno, L. Berthier, L. Cipelletti, G. Petekidis, and A. B. Schofield, Physical review letters **102**, 085703 (2009).
[2] G. Foffi, G. Savin, S. Bucciarelli, N. Dorsaz, G. M. Thurston, A. Stradner, and P. Schurtenberger, Proceedings of the National Academy of Sciences **111**, 16748 (2014).
[3] M. Tokuyama, Physical Review E **62**, R5915 (2000).
[4] L. M. Janssen, Frontiers in Physics **6**, 97 (2018).
[5] A. J. Hurd, D. W. Schaefer, and J. E. Martin, Physical Review A **35**, 2361 (1987).
[6] P. Bourrianne, V. Niggel, G. Polly, T. Divoux, and G. H. McKinley, Physical Review Research **4**, 033062 (2022).
[7] I. M. Krieger and T. J. Dougherty, Transactions of the Society of Rheology **3**, 137 (1959).
[8] D. Gilbert, R. Valette, and E. Lemaire, Journal of Rheology **66**, 161 (2022).
[9] D. Frenkel, R. Vos, C. De Kruif, and A. Vrij, The Journal of chemical physics **84**, 4625 (1986).
[10] F. Liénard, É. Freyssingeas, and P. Borgnat, The Journal of Chemical Physics **156**, 224901 (2022).

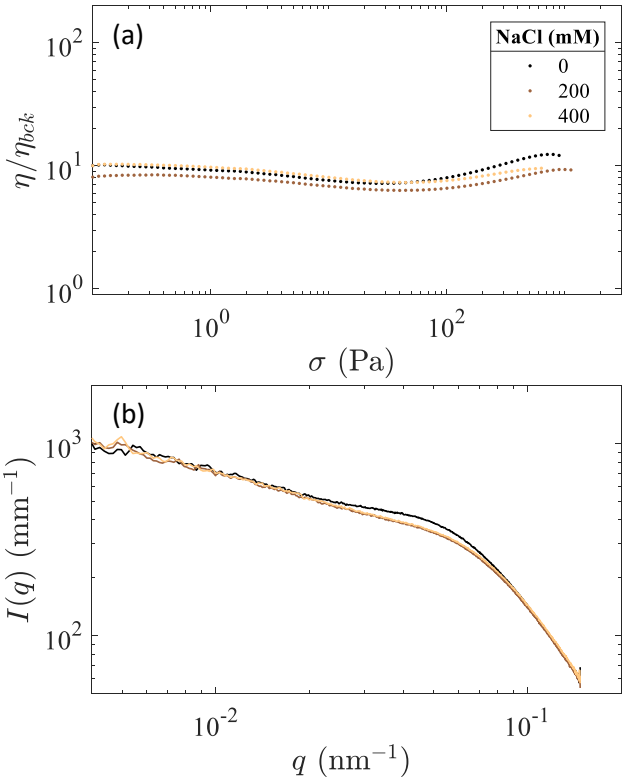

FIG. 7. . Influence of NaCl in fumed silica dispersion at $\phi = 0.098$. (a) Normalized viscosity as function of the shear stress. (b) Scattering intensity as a function of q